

Taylor & Francis
Taylor & Francis Group

Animal Cells and Systems

ISSN: 1976-8354 (Print) 2151-2485 (Online) Journal homepage: www.tandfonline.com/journals/tacs20

CD47-mediated purification of human ventricular cardiomyocytes derived from pluripotent stem cells

Soon-Jung Park, Hyung Kyu Choi, Keon Ha Park, Na Kyeong Park & Sung-Hwan Moon

To cite this article: Soon-Jung Park, Hyung Kyu Choi, Keon Ha Park, Na Kyeong Park & Sung-Hwan Moon (2026) CD47-mediated purification of human ventricular cardiomyocytes derived from pluripotent stem cells, Animal Cells and Systems, 30:1, 381-393, DOI: 10.1080/19768354.2026.2657637

To link to this article: https://doi.org/10.1080/19768354.2026.2657637

© 2026 The Author(s). Published by Informa UK Limited, trading as Taylor & Francis Group

View supplementary material

Published online: 20 Apr 2026.

Submit your article to this journal

Article views: 115

View related articles

View Crossmark data

Full Terms & Conditions of access and use can be found at
https://www.tandfonline.com/action/journalInformation?journalCode=tacs20

ANIMAL CELLS AND SYSTEMS
2026, VOL. 30, NO. 1, 381–393
https://doi.org/10.1080/19768354.2026.2657637

Taylor & Francis
by informa

OPEN ACCESS Check for updates

CD47-mediated purification of human ventricular cardiomyocytes derived from pluripotent stem cells

Soon-Jung Park [a,b*], Hyung Kyu Choi [b*], Keon Ha Park [b], Na Kyeong Park [b] and Sung-Hwan Moon [b]

[a]R&D Center, Biosolvix Co. Ltd, Seoul, Korea; [b]Department of Animal Science and Technology, Chung-Ang University, Anseong, Korea

ABSTRACT

Derivation of electrophysiologically mature cardiomyocytes from human pluripotent stem cells (hPSCs) remains a prerequisite for effective cardiac modeling and preclinical drug evaluation. However, current differentiation protocols often produce heterogeneous cell populations with limited maturity. In this study, we developed a CD47-based fluorescence-activated cell sorting strategy to purify ventricular-like cardiomyocytes from three-dimensionally differentiated hPSC-derived spheroids. $CD47^+$ cardiomyocytes exhibited highly consistent contractile behavior and enhanced structural maturation, as confirmed using immunocytochemistry for myosin regulatory light chain 2 ventricular/cardiac muscle isoform and α-actinin. Electrophysiological analysis using a patch clamp revealed that the majority of $CD47^+$ cells displayed ventricular-like action potential waveforms, characterized by prolonged repolarization duration, elevated amplitude, and a reduced negative maximum diastolic potential. Drug responsiveness was assessed using multi-electrode array recordings. CD47-enriched cardiomyocytes demonstrated reproducible and dose-dependent field potential alterations in response to known cardiotoxic agents, including remdesivir and quinidine, and outperformed metabolically purified controls in sensitivity and inter-replicate consistency analysis. These results establish CD47 as a reliable surface marker for isolating mature ventricular-like cardiomyocytes from hPSCs. The method enables the generation of functionally robust cardiomyocyte populations suitable for *in vitro* cardiac research and pharmacological testing.

ARTICLE HISTORY
Received 16 June 2025
Revised 28 February 2026
Accepted 6 April 2026

KEYWORDS
CD47; ventricular cardiomyocyte; surface marker-based purification; cardiotoxicity screening

Introduction

Cardiovascular diseases are among the leading causes of mortality worldwide and are closely associated with high attrition rates in drug development because of cardiotoxicity (Waring et al. 2015). In early-stage clinical trials, the inability to accurately predict adverse cardiac events often leads to trial failure and substantial financial losses (Paakkari 2002). Conventional preclinical models, such as two-dimensional cardiomyocyte cultures and animal models, have shown limited predictive power because they cannot replicate the structural, electrophysiological, and functional characteristics of the human heart (Ronaldson-Bouchard et al. 2018; Giacomelli et al. 2020).

Human pluripotent stem cell (hPSC)-derived cardiomyocytes offer a scalable and patient-relevant alternative for preclinical testing (Funakoshi et al. 2021). However, existing differentiation protocols frequently result in heterogeneous cell populations with variable degrees of maturity, limiting their utility in drug screening and disease modeling (Karbassi et al. 2020; Selvakumar et al. 2024). One strategy to overcome this limitation is to develop purification methods that selectively enrich mature cardiomyocyte subtypes, particularly those with ventricular-like properties that closely resemble the adult myocardium (Guo and Pu 2020).

CONTACT Sung-Hwan Moon moonsh@cau.ac.kr Department of Animal Science and Technology, College of Biotechnology and Natural Resources, Chung-Ang University Anseong, Gyeonggi-do, Republic of Korea
*These authors contributed equally to this study.

Supplemental data for this article can be accessed online at https://doi.org/10.1080/19768354.2026.2657637.

© 2026 The Author(s). Published by Informa UK Limited, trading as Taylor & Francis Group
This is an Open Access article distributed under the terms of the Creative Commons Attribution-NonCommercial License (http://creativecommons.org/licenses/by-nc/4.0/), which permits unrestricted non-commercial use, distribution, and reproduction in any medium, provided the original work is properly cited. The terms on which this article has been published allow the posting of the Accepted Manuscript in a repository by the author(s) or with their consent.

Several surface markers, including signal-regulatory protein alpha (SIRPA), vascular cell adhesion molecule 1 (VCAM1), and CD71, have been explored to isolate hPSC-derived cardiomyocytes using fluorescence-activated cell sorting (FACS), but these approaches often result in populations with inconsistent electrophysiological and functional profiles (Dubois et al. 2011; Uosaki et al. 2011; Boheler and Poon 2021). In addition, metabolic purification methods – such as lactate-based purification – have shown utility but also yield heterogeneous outcomes (Tohyama et al. 2013).

In this study, we investigated CD47 as a surface marker for the purification of cardiomyocytes derived from hPSCs. CD47 is a transmembrane protein traditionally considered to be involved in immune modulation (Deuse et al. 2021); however, recent evidence suggests that CD47 is stably expressed in ventricular-like cardiomyocytes (Veevers et al. 2018). Our electrophysiological analysis confirmed that CD47-positive cells display action potential profiles characteristic of mature ventricular cardiomyocytes, including prolonged repolarization and stabilized depolarization kinetics. We developed a FACS-based purification protocol using CD47 to isolate high-purity cardiomyocytes from three-dimensional (3D)-differentiated hPSC-derived spheroids. The purified cells were evaluated to determine their contraction consistency, electrophysiological properties, and *in vitro* maturation potential. This study highlights the utility of CD47 as a functional marker to enrich physiologically relevant cardiomyocytes and provides a refined *in vitro* model system for cardiotoxicity assessment and cardiac research.

Materials & methods

3D differentiation of cardiomyocytes from hiPSCs

Human induced pluripotent stem cells (hiPSCs, BS-hiPSC-05; ACE-hiPSC-02) were used in this study. BS-hiPSC-05 was reprogrammed from dermal fibroblasts using mRNA-based transfection and was validated for pluripotency marker expression, mycoplasma negativity, and a normal karyotype (Supplementary Figure 1). In addition, the ACE-hiPSC-02 line, which has been utilized in previous independent studies, was included to demonstrate the reproducibility of our purification across distinct cell sources (Park et al. 2025).

hiPSCs were cultured on vitronectin-coated dishes (Gibco, A14700) in StemMACS iPS-Brew XF medium (Miltenyi Biotec, 130-091-680) supplemented with 10 ng/mL epidermal growth factor (EGF; R&D Systems, 236-EG) and 10 μM Y27632 (Tocris, 1254) for 24 h after passage. Upon reaching approximately 90% confluence, the cells were dissociated by adding 0.5 mM EDTA (Gibco, Thermo Fisher, R1021) and seeded at a density of 1×10^4 cells per well into round-bottom, Pluronic F-127-coated 96-well plates (Sigma-Aldrich, P2443) to promote spheroid formation. Spheroids were formed over 3 days (days 1–4) in basal medium supplemented with 10% N2 supplement (Gibco, 17502048) and 8% fetal bovine serum (FBS; Hyclone, SH30071.03). On day 4, the spheroids were transferred to a medium containing 12 ng/mL of bone morphogenetic protein 4 (BMP4, R&D Systems, 314-BP) and 8% FBS to induce the mesodermal lineage. After 48 h (day 6), the medium was replaced with medium containing 20% FBS to promote cardiac specification; the medium was refreshed on day 8. From day 10, the medium was replaced with medium supplemented with 10% FBS and refreshed again on day 12. Spontaneous beating was typically observed from day 10 onward, and differentiated spheroids were harvested on day 14.

Flow cytometry and CD47-based cardiomyocyte purification

Beating cardiomyocyte spheroids harvested on day 14 of differentiation were dissociated into single cells using TrypLE Express (Gibco, A1217702) at 37°C for 10 min. The resulting cell suspension was washed twice with phosphate-buffered saline (Welgene, LB001-02) and passed through a 40 μm cell strainer (SPL Life Sciences, 93040) to obtain a single-cell population. For surface marker staining, the cells were incubated with phycoerythrin/cyanine7-conjugated anti-human CD47 antibody (BioLegend, 323108; 1:100) for 30 min at 4°C. Subsequently, the cells were fixed and permeabilized using the BD Cytofix/Cytoperm™ Fixation/Permeabilization Kit (BD Biosciences, 554655) for 15 min, followed by intracellular staining with Alexa Fluor® 488-conjugated mouse anti-cardiac troponin T (cTnT) antibody (BD Biosciences, EPR20266; 1:50) for 30 min at 4°C. Stained cells were resuspended in phosphate-buffered saline containing

5% FBS and analyzed using a SH800S Cell Sorter (Sony Biotechnology). Data were processed using Cell Sorter Software Ver 2.1.5 (Sony Biotechnology) to evaluate the expression of CD47 and cTnT, and to isolate $CD47^+$ cardiomyocytes.

Immunofluorescence

hiPSC-cardiomyocytes were plated onto gelatin-coated glass dishes and cultured for 5 days. The cells were fixed with 4% paraformaldehyde (Biosesang, P2031) for 20 min at 4°C, permeabilized with 0.1% Triton X-100 (Merck, 112298) for 10 min at 20°C, and blocked with 0.03% Triton X-100 containing 10% normal goat serum for 30 min at room temperature. These cells were stained with monoclonal antibodies against cTnT (Invitrogen, MA5-12960) (1:500), CD31 (R&D Systems, AF3628) (1:200), and sarcomeric-α-actinin (Abcam, ab137346) (1:200) diluted in 0.03% Triton X-100 and incubated at 4 °C overnight. The cells were washed three times for 10 min with 0.03% Triton X-100 and incubated with, Alexa Fluor™ 488 (Invitrogen) goat anti-mouse IgG (H + L) cross-adsorbed secondary antibody (Invitrogen, A-11001, 1:200), and Alexa Fluor 594 (Invitrogen) antibodies (Invitrogen, A-11012, 1:200) for 1 h at room temperature. The cells were washed four times before counterstaining the cell nuclei with DAPI Staining Solution (Sigma-Aldrich, D9542). All images were analyzed using a Ti2 fluorescence microscope (Nikon).

Contraction analysis of purified cardiomyocytes

CD47-purified and metabolic-based purified cardiomyocytes were seeded onto Matrigel-coated 24-well plates at 5×10^4 cells/well. (Corning, 354234) $CD47^+$ cells were obtained via flow cytometry following antibody staining. Metabolically purified cells were cultured in glucose-free RPMI 1640 medium (Thermo Fisher Scientific, 11879020) supplemented with 5 mM sodium DL-lactate (Sigma-Aldrich, 71720), whereas CD47-purified cells were maintained in RPMI 1640 containing 5% FBS. In this approach, cardiomyocytes survived by utilizing lactate through mitochondrial metabolism, whereas non-cardiomyocytes with limited mitochondrial function underwent cell death, resulting in selective enrichment of cardiomyocytes.

The medium was replaced every 3 days. Three days after seeding, spontaneous beating was confirmed. Five representative beating cardiomyocytes were selected per group, and 1-min brightfield videos were recorded at 4× and 10× magnification using the Ti2 microscope. Contraction intervals and beats per minute (BPM) were manually quantified using ImageJ software (ver 1.54k) based on visible contraction-relaxation cycles.

Sarcomere length analysis

Metabolically purified and CD47-purified cardiomyocytes were immunostained with a monoclonal antibody against sarcomeric-α-actinin (1:200), followed by incubation with Alexa Fluor™ 488 goat anti-mouse IgG (H + L) secondary antibody (Invitrogen, A-11008). Confocal fluorescence images were acquired at 180× magnification using identical settings for all samples. The sarcomere length was quantified from α-actinin – stained images using FIJI (ImageJ) by measuring the distance between adjacent Z-lines along the longitudinal axis of cardiomyocytes. Multiple sarcomeres were analyzed per cell, and the mean sarcomere length was calculated for each of the four biological replicates per group (n = 4) for statistical comparison.

Electrophysiological analysis (Patch clamp)

Electrophysiological recordings were performed at physiological temperature (37°C) using an external solution composed of 130 mM NaCl, 5 mM KCl, 1 mM $MgCl_2$, 1.8 mM $CaCl_2$, 10 mM HEPES, and 12.5 mM glucose, with the pH adjusted to 7.4. Patch clamp measurements were conducted using glass micropipettes filled with an internal solution containing 120 mM potassium aspartate, 20 mM KCl, 10 mM HEPES, 5 mM EGTA, 1 mM $MgCl_2$, and 1.5 mM Mg-ATP, adjusted to pH 7.3. Membrane currents were recorded using an Axopatch 200B amplifier connected to a Digidata 1440A digitizer, and data were acquired and analyzed using pClamp software (Molecular Devices). Voltage clamp protocols involved holding cells at – 80 mV, followed by depolarization to +40 mV for 4 s and then repolarization to –40 mV for 2 s.

Drug treatment and multi-electrode array-based electrophysiological recording

To evaluate drug-induced electrophysiological responses, CD47-purified cardiomyocytes and metabolic-based purified cardiomyocytes were cultured as monolayers on fibronectin-coated 96-well multi-electrode array (MEA) plates (CytoView; Axion BioSystems). The cells were maintained in RPMI 1640 medium supplemented with B27 (Gibco, 17504044) until stable spontaneous beating was observed. Field potentials generated by spontaneous beating were recorded using the Maestro Pro MEA system (Axion BioSystems). Prior to drug exposure, baseline signals were recorded. The drugs, remdesivir (MedChemExpress, HY-104077) and quinidine (Sigma-Aldrich, Q3625), were diluted by 10× in culture medium and added to each well at 10% (v/v) to achieve final concentrations of 10 or 30 μM for remdesivir and 9.5 μM for quinidine. Each well received a single drug concentration. Electrophysiological changes were monitored over a 30-min period following drug administration. Two independent 5-min recordings were performed for each well to assess post-treatment effects. All experiments were conducted in triplicate. As field potential parameters, the field potential duration (FPD), beat interval, and amplitude were extracted using the Cardiac Analysis Tool and AxiS Metric Plotting Tool software (Axion BioSystems).

Statistical analysis

Data are expressed as the means ± standard error of the mean (SEM). Unpaired two-tailed Student's *t*-test was used to compare two groups. $P < 0.05$ was considered statistically significant.

Results

Differentiation of cardiomyocytes through spheroid formation

To generate 3D cardiomyocytes from hiPSCs, human iPSCs were subjected to a stepwise spheroid-based protocol consisting of five distinct stages, as schematically illustrated in Figure 1(A). During stage 1, undifferentiated hiPSCs were seeded onto vitronectin-coated plates and primed with Y-27632 and EGF to support initial survival and expansion. In stage 2, dissociated cells were transferred to low-adhesion, Pluronic F-127-coated plates to facilitate the formation of uniform spheroids under serum- and N2-supplemented conditions.

By day 4, spheroid formation was complete, and subsequent treatment with BMP4 (stage 3) induced mesodermal lineage commitment. During stages 4 and 5 (days 6–14), FBS-enriched culture medium was used to promote cardiac specification and maturation. Notably, spontaneous contractile activity was first observed around day 10 and progressively increased, with most spheroids exhibiting rhythmic and coordinated beating by day 14, indicative of functional cardiomyocyte generation. Representative microscopic images captured during stages 4 and 5 confirmed morphological compaction and contraction-competent spheroid structures (Figure 1(A)).

Purification of cardiomyocytes using the CD47 surface marker

To evaluate the efficiency of cardiomyocyte purification using CD47 as a surface marker, we first established a 3D differentiation protocol from hPSCs. As illustrated in Figure 1(A), the protocol was divided into five stages spanning 14 days, incorporating temporal supplementation with Y-27632, EGF, N2, BMP4, and FBS to induce spheroid formation and cardiomyocyte maturation. Representative bright-field images revealed the morphological changes occurring during each stage of differentiation.

Flow cytometry was performed on single-cell suspensions derived from day-14 beating spheroids to assess marker expression before and after CD47-based sorting. Prior to sorting, 79.74% of the population expressed surface CD47 (Figure 1(B)) and 58.67% stained positive for the intracellular cardiomyocyte marker cTnT (Figure 1(C)), indicating a partially differentiated, heterogeneous population. Following FACS using phycoerythrin/cyanine7-conjugated anti-CD47 antibody, the $CD47^{+}$ population was enriched to 96.28% (Figure 1(D)). Among these sorted cells, 99.89% were also cTnT-positive (Figure 1(E)), confirming the successful isolation of cardiomyocytes with high purity.

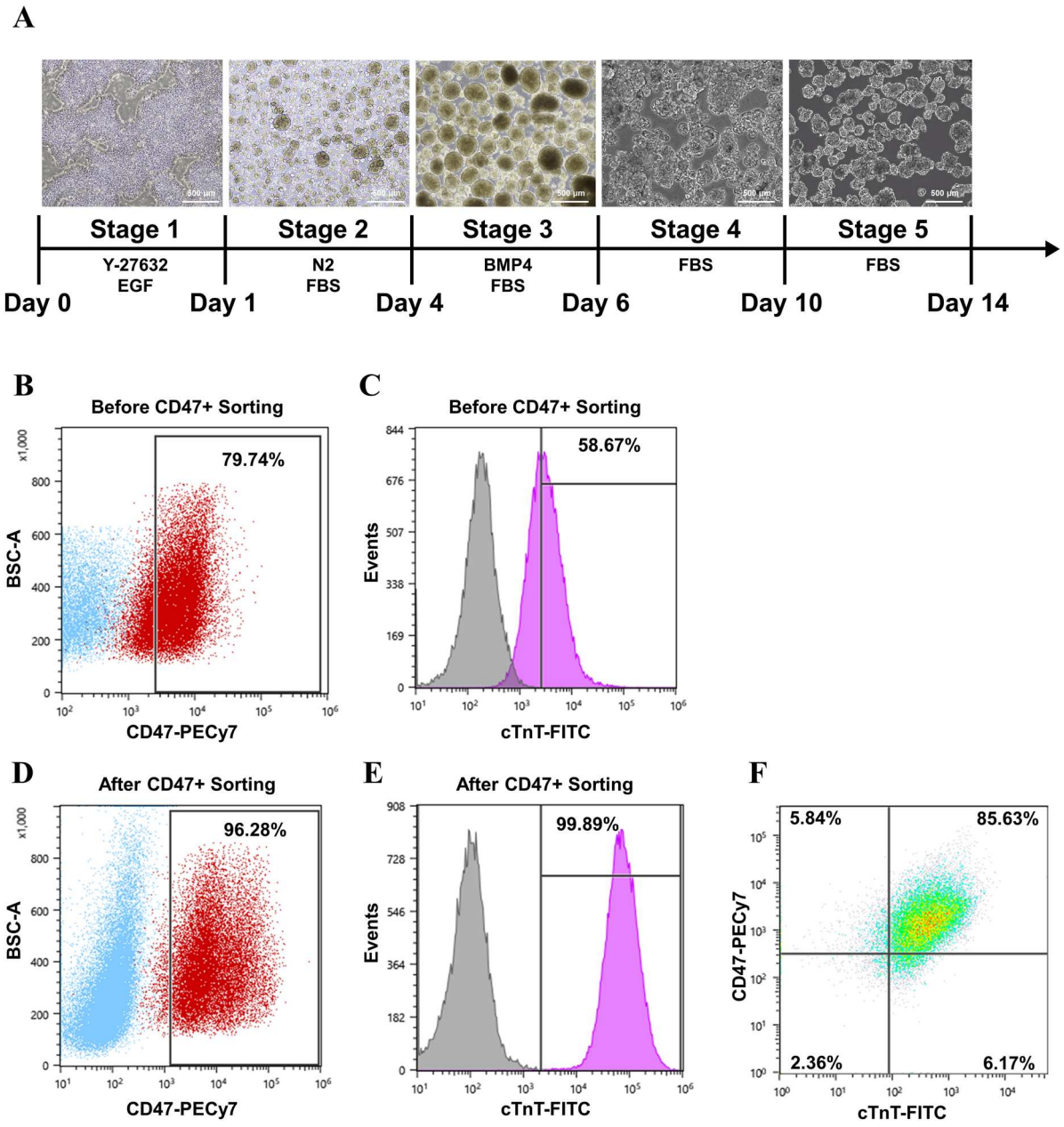


Figure 1. Schematic of 3D cardiomyocyte differentiation and FACS-based purification using CD47 (A) Schematic protocol for 3D differentiation of cardiomyocytes from human pluripotent stem cells. The differentiation process is divided into five stages over 14 days, utilizing temporal supplementation of Y-27632, EGF, N2, BMP4, and FBS to guide spheroid formation and cardiomyocyte maturation. Representative bright-field images show the morphological changes during each stage. (B – E) Flow cytometry analysis of differentiated cells before (B, C) and after (D, E) CD47-based sorting. Prior to sorting, 79.74% of cells expressed CD47 (B), and 58.67% were positive for the cardiomyocyte marker cTnT (C). After sorting, the CD47 + cell population increased to 96.28% (D), and cTnT + cells accounted for 99.89% of the total (E), indicating successful enrichment of cardiomyocytes. (F) Dual-marker analysis post-sorting demonstrated that 85.63% of the CD47 + sorted population co-expressed both CD47 and cTnT, supporting the utility of CD47 as an effective surface marker for cardiomyocyte purification. Abbreviations: cTnT, cardiac troponin T; FACS, fluorescence-activated cell sorting; FITC, fluorescein isothiocyanate; PE, phycoerythrin. All images were captured using a microscope (4×).

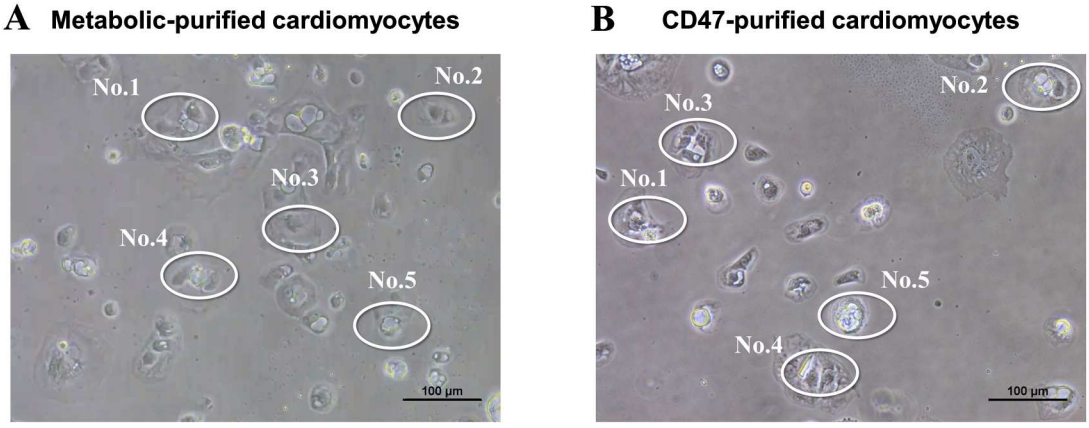
To further assess the correlation between CD47 and cardiomyocyte identity, dual-marker flow cytometric analysis was performed. As shown in Figure 1 F, 85.63% of the post-sorted population co-expressed CD47 and cTnT. Only minor fractions of the cells were $CD47^{-}/cTnT^{-}$ (2.36%), $CD47^{+}/cTnT^{-}$ (5.84%), or $CD47^{-}/cTnT^{+}$ (6.17%). This result highlights the specificity of CD47 expression for cardiomyocytes within the differentiated population.

To confirm the robustness and reproducibility of the CD47-based purification protocol, we repeated the experiment using an independently differentiated hiPSC line (ACE-hiPSC-2). In this validation experiment, CD47-sorted cells exhibited similar high purity, confirming that CD47 provides a reliable and reproducible surface marker for enriching cardiomyocytes across different hiPSC sources (Supplementary Figure 2).

Evaluation of contraction capability in purified cardiomyocytes

Optical microscopy was performed to confirm the consistent contraction ability of cardiomyocytes purified using the CD47 surface marker. The contraction capability of these cells was compared to that of cardiomyocytes purified using the conventional metabolic-based method.

The CD47-based purification method isolates cardiomyocytes expressing the CD47 surface marker through flow cytometry, whereas the metabolic-based method involves culturing cells in medium devoid of D-glucose and supplemented with lactate. In the metabolic-based approach, cardiomyocytes survive because their mitochondria can utilize lactate as an energy source, whereas non-cardiomyocytes with fewer mitochondria undergo cell death, resulting in selective purification of cardiomyocytes (Tohyama et al. 2013; Kadari et al. 2015; Ban et al. 2017; Laco et al. 2020). For the metabolism-based method, day-14 beating spheroids were dissociated into single cells using TrypLE and seeded onto Matrigel-coated plates but cultured in glucose-free medium supplemented with lactate, with the medium also replaced every 3 days (Figure 2(A)). For CD47-



C

No.	Interval (s)		Contracting No (1 min)	
	Metabolic	CD47	Metabolic	CD47
1	1.25	1.43	48	42
2	1	1.25	60	48
3	1.30	1.50	46	40
4	0.91	1.36	66	44
5	1.20	1.58	50	38
Interval (Gap)	**0.91-1.30** (0.39)	**1.25-1.58** (0.33)	**46-66** (20)	**36-48** (12)

Figure 2. Comparison of cardiomyocyte contraction intervals and frequency between metabolic-purified and CD47-purified cardiomyocytes (A) Representative images of metabolic-purified and (B) CD47-purified cardiomyocytes. The numbered regions (No. 1 to No. 5) indicate the areas where contraction events were measured. (C) Comparison of contraction intervals and frequency between metabolic-purified and CD47-purified cardiomyocytes. CD47-purified cells showed more consistent contraction intervals and frequencies compared to metabolic-purified cells, with narrower variation in both metrics. All images were captured using a microscope (10×).

based purification, cardiomyocytes isolated via flow cytometry were seeded onto Matrigel-coated culture plates and maintained in a medium supplemented with 5% FBS. The medium was replaced every 3 days (Figure 2(B)). Beating cardiomyocytes were observed in both groups 3 days after seeding (Supplementary Videos 1 and 2). Five representative beating cardiomyocytes were selected from each group for further analysis (Figure 2(A,B)).

The contraction intervals and BPM of the selected cells were measured for 1 min using optical microscopy (Figure 2(C)). For metabolic-based purified cardiomyocytes, contraction intervals ranged from 0.91–1.30 s, with a variation of 0.39 s among the five selected cells. In contrast, CD47-purified cardiomyocytes exhibited contraction intervals of 1.25–1.58 s, with a much smaller variation of 0.33 s among the five cells. Metabolic-based purified cells showed a range of 46–66 BPM, with a variation of 20 BPM among cells. In comparison, CD47-purified cardiomyocytes demonstrated a more consistent range of 36–48 BPM, with a variation of only 12 BPM.

Electrophysiological analysis of CD47 surface marker-purified cardiomyocytes

To analyze the electrophysiological properties of cardiomyocytes purified using the CD47 surface marker, evaluations were conducted using the patch clamp technique. The electrophysiological analysis of cardiomyocytes revealed three types of action potentials (APs) in the heart: nodal-like, atrial-like, and ventricular-like (Figure 3(A)). Electrophysiological analysis was performed on 40 single cardiomyocytes, and quantitative analyses of the amplitude, action potential during 80% repolarization (APD80), upstroke velocity (Vmax), maximum diastolic potential (MDP), and beat period were conducted for atrial-like and ventricular-like cells, excluding nodal-like cells, which are characterized by unstable membrane potentials and low electrical activity. After analyzing the electrophysiological properties for each indicator using the patch clamp technique, the cells were categorized into atrial – or ventricular-like types, and the mean values were calculated (Figure 3(B)). The results of patch clamp analysis showed that the 40 cardiomyocytes consisted of 75% ventricular-like cells, 20% atrial-like cells, and 5% nodal-like cells (Figure 3(C)).

Among the three types of cells in the heart, ventricular-like cells, characterized by highly negative MDP values, long APDs, high amplitudes, and high Vmax values, represent the features of mature cardiomyocytes. A larger proportion of ventricular-like cells is indicative of a more mature cardiomyocyte model. Electrophysiological analysis using the patch clamp technique confirmed that cardiomyocytes purified using the CD47 surface marker were predominantly composed of ventricular-like cells.

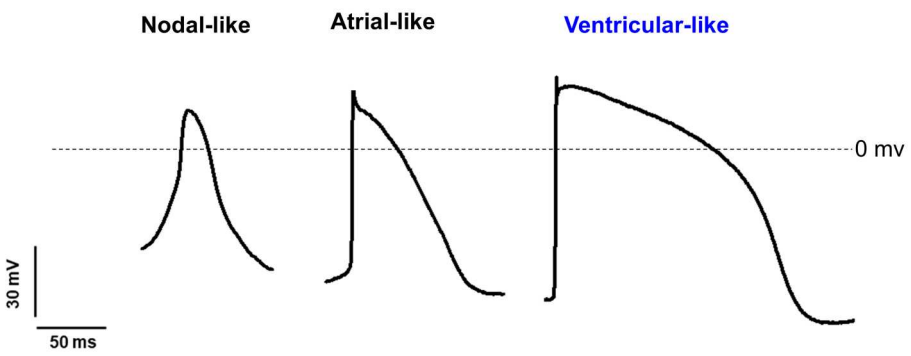
Maturation of CD47 surface marker-purified cardiomyocytes

To analyze the maturation of cardiomyocytes purified via the CD47 surface marker, morphological changes and contraction patterns were assessed using optical microscopy. Cardiomyocytes purified using the CD47 surface marker and seeded onto Matrigel-coated culture plates initially displayed short and irregular contraction intervals, with a small cell surface area (Supplementary Videos 3 and 4). After 2 weeks of maturation, the cardiomyocytes exhibited regular and elongated contraction intervals, along with an increased cell surface area (Supplementary Videos 5 and 6).

Immunofluorescence staining was performed to confirm the maturation status of the CD47-purified cardiomyocytes. DAPI was used to stain the nuclei, and the cardiac-specific markers sarcomeric-α-actinin and myosin light chain 2, ventricular/cardiac muscle isoform (MLC2v) were stained at wavelengths of 594 and 488 nm, respectively. Sarcomeric-α-actinin, which is increasingly expressed in mature cardiomyocytes, highlights well-defined Z-line structures in sarcomeres. MLC2v, a marker specific to ventricular-like cardiomyocytes, was used to assess cardiomyocyte maturation. Immunofluorescence analysis revealed clear sarcomeric structures through sarcomeric-α-actinin expression and confirmed cardiomyocyte maturation via MLC2v expression in the CD47-purified cells (Figure 4(A)).

To further evaluate morphological and structural maturation, CD47-purified cardiomyocytes were examined before and after a 2-week *in vitro* maturation period using both bright-field microscopy and immunofluorescence. Bright-field images revealed a clear morphological shift, with cells becoming larger and more elongated after 2 weeks of culture in maturation-promoting medium (Figure 4(B), upper panel). This

A



B

	Amplitude (mV)	APD 80 (ms)	Vmax (mV/ms)	MDP (mV)	Beat period (ms)
Atrial-like hiPSC-CMs	85.21 ± 7.25	131.66 ± 18.41	28.95 ± 6.20	-58.11 ± 3.46	234.08 ± 65.82
Ventricular like hiPSC-CMs	109.13 ± 9.43	220.43 ± 15.60	43.27 ± 9.32	-69.10 ± 5.61	648.97 ± 81.20

C

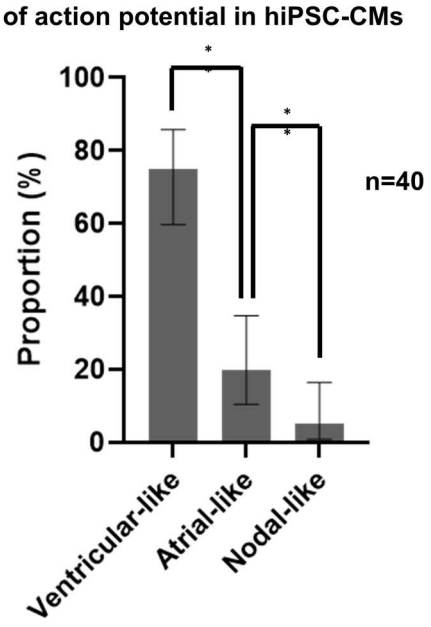


Figure 3. Electrophysiological analysis of CD47-purified cardiomyocytes using the patch clamp technique (A) Representative AP waveforms of the three cardiac cell types: nodal-, atrial-, and ventricular-like cardiomyocytes are shown. (B) Quantitative comparison of electrophysiological parameters, including amplitude, APD80, Vmax, MDP, and beat period for atrial – and ventricular-like cardiomyocytes is presented. Ventricular-like cells showed a higher amplitude, longer APD80, greater Vmax, more negative MDP, and slower beat period, indicative of mature cardiomyocyte properties. (C) Proportional distribution of cardiac cell types in CD47-purified cardiomyocytes is illustrated. Among the 40 analyzed cells, 75% were ventricular-like, 20% were atrial-like, and 5% were nodal-like, reflecting the prevalence of ventricular-like cells in the purified population. The higher proportion of ventricular-like cells with mature electrophysiological features supports the effectiveness of CD47-purification in isolating mature cardiomyocytes. Data are presented as the mean ± SEM. Error bars represent the 95% confidence interval (95% CI) for each cell type proportion. Statistical significance was determined using unpaired two-tailed Student's *t*-test (*$p < 0.05$; **$p < 0.01$). Abbreviations: AP, action potential; APD80, action potential during 80% repolarization; CM, cardiomyocytes; hiPSC, human induced pluripotent stem cell; MDP, maximum diastolic potential; Vmax, maximum upstroke velocity.

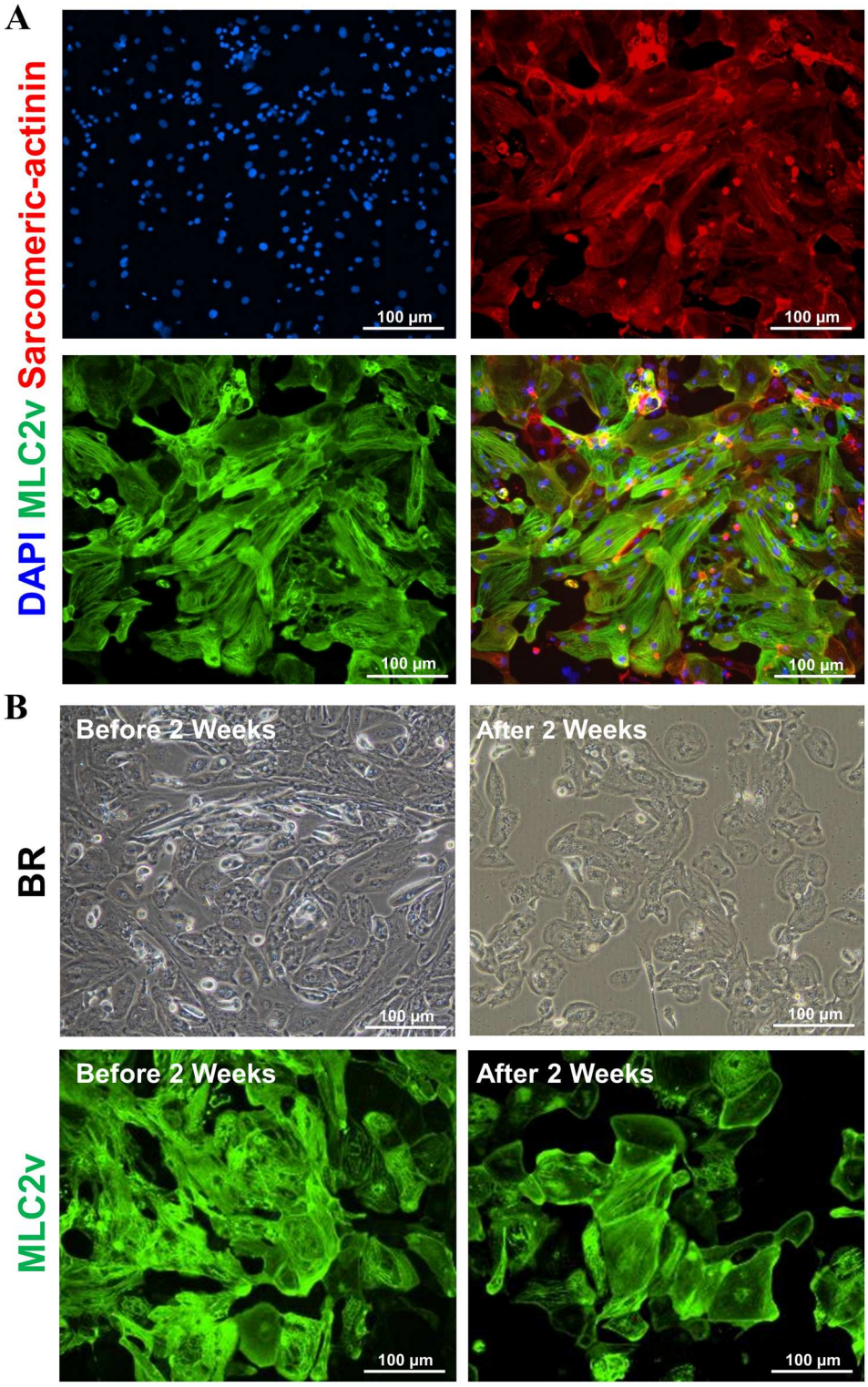


Figure 4. Morphological and immunofluorescent analysis of CD47-purified cardiomyocytes during maturation (A) Immunocytochemistry analysis of cardiomyocytes purified using CD47-based FACS. Cells were stained with cardiac-specific markers: MLC2v (green) and sarcomeric α-actinin (red), with nuclei counterstained by DAPI (blue). Co-expression of MLC2v and sarcomeric α-actinin confirms the cardiomyocyte identity of CD47-purified cells. (B) BR and MLC2v immunofluorescence images of CD47-purified cardiomyocytes before (left column) and after (right column) 2 weeks of *in vitro* maturation in basal medium supplemented with 20% N2 supplement and 5% fetal bovine serum. After 2 weeks, cells exhibit increased cell spreading and surface area, suggesting morphological maturation. These results indicate that CD47 + purified cells were functional cardiomyocytes capable of further maturation. ICC images were captured using a confocal microscope (10×) and BR images were captured using a microscope (10×). Abbreviations: BR, bright-field; FACS, fluorescence-activated cell sorting; ICC, Immunocytochemistry.

transition was accompanied by a reduction in intercellular spacing and increased cellular alignment. Immunofluorescence analysis of MLC2v confirmed the cardiac identity of the cells at both time points (Figure 4(B), lower panel). However, post-maturation cardiomyocytes displayed a more intense and spatially organized MLC2v signal, consistent with enhanced structural maturity. These results suggest that extended culture promotes the morphological and molecular maturation of CD47-purified ventricular cardiomyocytes, supporting their suitability for downstream functional applications.

In addition to qualitative assessments, quantitative analyses were incorporated to evaluate enhanced maturation in CD47-purified cardiomyocytes. Sarcomere length, a widely accepted structural index of cardiomyocyte maturation, was measured using high-resolution immunofluorescence imaging (Supplementary Figure 3). CD47-purified cardiomyocytes exhibited significantly longer sarcomeres than did metabolically purified cells ($p < 0.01$), consistent with the presence of more organized and mature contractile units. This quantitative increase in sarcomere length supports the morphological and molecular maturation features observed in MLC2v expression and cellular morphology. Together, these results directly address quantitative maturation metrics and further substantiate that CD47-based purification yields a structurally more mature ventricular cardiomyocyte population.

Analysis of drug-induced changes in CD47 surface marker-purified cardiomyocytes

To evaluate the cardiotoxic effects of drugs on CD47-purified cardiomyocytes, the MEA technique was employed to analyze electrophysiological changes in cardiomyocytes. MEA enables the measurement of the field potential duration, beat interval, and amplitude before and after drug treatment (Figure 5(A)).

The cardiomyocytes used for drug evaluation included CD47-purified cardiomyocytes and metabolic-based purified cardiomyocytes as a comparison group. Each type of cardiomyocyte, cultured in two dimensions, was treated with remdesivir and quinidine to assess drug toxicity. At a remdesivir concentration of 10 μM, CD47-purified cardiomyocytes exhibited a greater reduction in field potential amplitude than did metabolism-based purified cardiomyocytes, indicating higher sensitivity to remdesivir-induced electrophysiological suppression (Figure 5(B)). However, at a remdesivir concentration of 30 μM, both groups exhibited toxic responses to remdesivir. For quinidine, both cell populations showed amplitude decreases at 9.5 μM (Figure 5(C)). However, the reduction was more pronounced in CD47-purified cardiomyocytes, demonstrating clearer sensitivity to quinidine-induced electrophysiological perturbation. This heightened responsiveness in the CD47-purified group is consistent with the clinically recognized proarrhythmic risk of quinidine at near-therapeutic levels.

Discussion

We developed a CD47-based purification strategy to isolate functionally mature cardiomyocytes derived from hPSCs. CD47 is widely expressed in cardiac tissue and participates in cell – cell signaling and stress-associated pathways (Sharifi-Sanjani et al. 2014), providing biological plausibility for its use as a surface phenotype for cardiomyocyte enrichment. Using FACS, CD47-based sorting yielded cardiomyocytes exhibiting ventricular-like electrophysiological characteristics with consistent contraction behavior and reduced variability in drug responses, supporting its utility for cardiac modeling and preclinical screening.

Compared with metabolic purification, CD47-based selection provided superior electrophysiological uniformity. Lactate-based purification remains one of the most widely adopted strategies because of its simplicity and scalability (Tohyama et al. 2013). However, glucose deprivation and lactate-enriched conditions impose metabolic stress that may alter cellular bioenergetics or introduce phenotypic variability (Ban et al. 2017; Rupert et al. 2020). Because CD47 purification relies on surface phenotype rather than metabolic conditioning, it avoids potential physiological artifacts associated with nutrient withdrawal and yields a more consistent ventricular-like population.

$CD47^+$ cardiomyocytes predominantly exhibited ventricular-like action potential profiles, including prolonged APD80, increased Vmax, more negative maximum diastolic potential, and greater action potential amplitude, which are all hallmarks of electrophysiological maturation. These findings indicate that CD47 can be used as a phenotypic enrichment marker for ventricular-like cardiomyocytes. Importantly, CD47 is not known to mechanistically regulate chamber specification or electromechanical maturation, and no

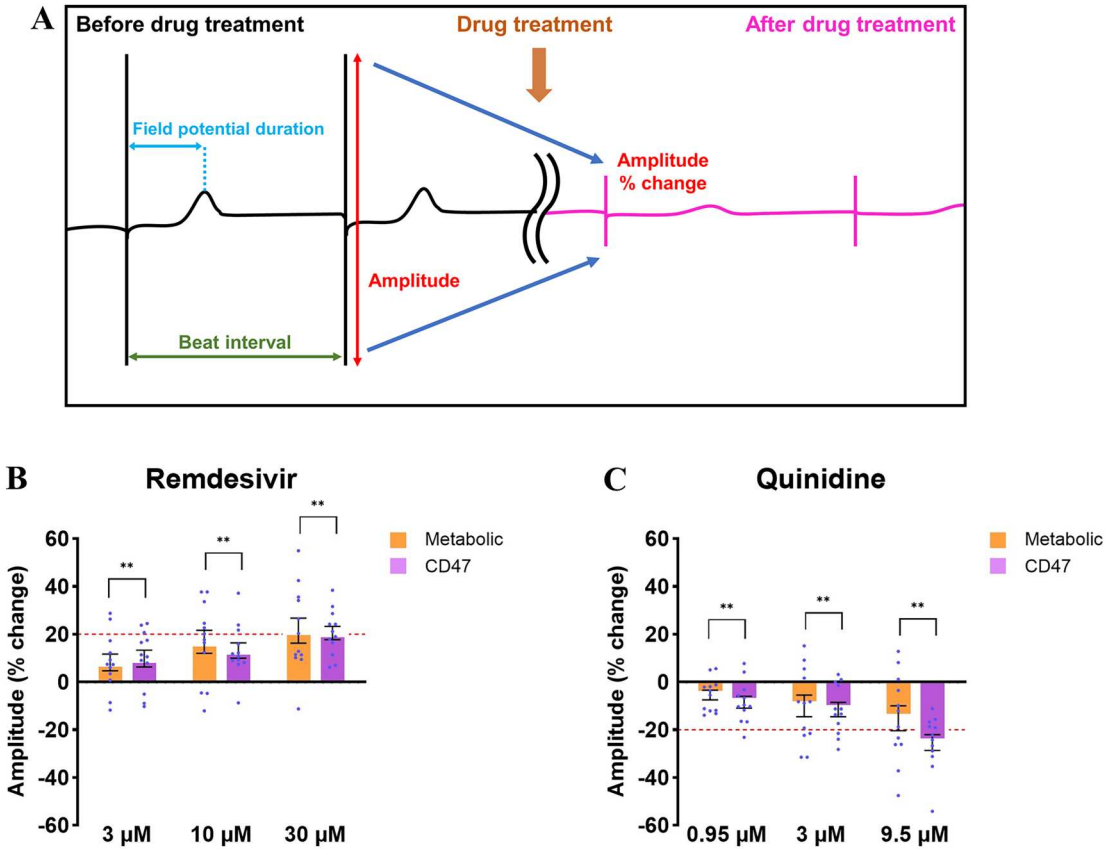


Figure 5. Drug toxicity sensitivity comparison between metabolic-purified and CD47-purified cardiomyocytes (A) Schematic representation showing changes in field potential amplitude before and after drug treatment. Beat interval and amplitude were measured to assess cardiomyocyte response to drugs. (B) Bar graph displaying the percentage change in amplitude after treatment with remdesivir at different concentrations. CD47-purified cardiomyocytes (purple) showed greater sensitivity to remdesivir-induced changes in amplitude compared to metabolic-purified cells (orange), particularly at higher concentrations (10 μM). (C) Bar graph showing the percentage change in amplitude after treatment with quinidine. CD47-purified cardiomyocytes (purple) exhibited significantly higher sensitivity to drug-induced amplitude reduction, especially at 9.5 μM, compared to metabolic-purified cells (orange). Data are presented as the mean ± SEM, with individual data points shown. Sample size: n = 12 recordings per group. Statistical significance was determined using unpaired two-tailed Student's *t*-test (*$p < 0.05$; **$p < 0.01$).

molecular evidence to date supports a causal relationship between CD47 expression and ventricular identity. Accordingly, the interpretations presented here are limited to phenotypic correlation rather than to mechanistic inference.

To address concerns regarding variability between cell lines, we validated CD47 surface expression and sorting performance using a second independently differentiated hiPSC line (ACE-hiPSC-2). CD47-based purification consistently yielded ≥95% $CD47^+$ cells in this line, demonstrating that the surface-marker phenotype and purification efficiency are robust across distinct genetic backgrounds.

Structural maturation analysis further supported the electrophysiological findings. $CD47^+$ cardiomyocytes exhibited significantly increased sarcomere length, enhanced sarcomeric organization, and elevated MLC2v expression, all of which are established markers of ventricular-like cardiomyocyte subtype and maturation (Cai et al. 2019; Gao et al. 2023). Together, these data indicate that CD47-based sorting enriches both the structural and functional hallmarks of mature ventricular cardiomyocytes.

CD47 sorting offers complementary advantages over existing purification methods. Surface-marker – based methods such as SIRPA and VCAM1 have demonstrated utility for isolating broad cardiomyocyte populations (Dubois et al. 2011; Uosaki et al. 2011), with VCAM1 specifically associated with more structurally mature lineages (Skelton et al. 2014). However, both markers capture heterogeneous cardiomyocyte subtypes. In contrast, CD47 sorting enriches a narrower but more functionally coherent ventricular-like

population, yielding reduced electrophysiological variability, although with slightly lower overall cell recovery. CD47 should therefore be considered a complementary strategy prioritizing electrophysiological fidelity and subtype specificity over maximal yield.

Drug response analyses further highlighted these advantages, demonstrating that CD47-purified cardiomyocytes displayed more reproducible and clinically consistent responses to remdesivir and quinidine than those by metabolically purified cells. The ability to reliably generate ventricular-like cardiomyocytes with high physiological fidelity could support the development of engineered cardiac tissues aligned with FDA-endorsed New Approach Methods frameworks for preclinical safety testing (Administration 2025).

In conclusion, our CD47-based purification strategy enables scalable and reproducible enrichment of ventricular-like cardiomyocytes with high functional consistency across multiple hPSC lines. Although the mechanistic role of CD47 in subtype specification remains undefined, our findings establish CD47 as a robust correlation-based phenotypic marker that enhances the precision of *in vitro* cardiac modeling, pharmacological testing, and tissue engineering applications.

Disclosure statement

No potential conflict of interest was reported by the author(s).

Funding

This work was supported by the Korean Fund for Regenerative Medicine (KFRM) grant funded by the Ministry of Science and ICT, the Ministry of Health & Welfare 25A0203L1; the Bio&Medical Technology Development Program of the National Research Foundation under Grant RS-2023-00220207; and supported by a grant (26212MFDS166) from Ministry of Food and Drug Safety in 2026.

Ethical statement

This study was approved by the Institutional Review Board (IRB) of Kyungpook National University Hospital, Kyungpook National University (IRB approval number: KNUH IRB 2023-12-002-002). Informed consent was obtained from all participants after the nature and possible consequences of the study had been fully explained to them.

Data availability statement

The data will be made available on request.

ORCID

Soon-Jung Park http://orcid.org/0000-0002-9384-6034
Hyung Kyu Choi http://orcid.org/0009-0002-7329-9261
Keon Ha Park http://orcid.org/0009-0007-5247-4426
Na Kyeong Park http://orcid.org/0000-0002-6903-3068
Sung-Hwan Moon http://orcid.org/0000-0003-1858-0261

References

Administration, U. S. F. A. D. 2025. FDA announces plan to phase out animal testing requirement for monoclonal antibodies and other drugs. Retrieved May 9 from https://www.fda.gov/news-events/press-announcements/fda-announces-plan-phase-out-animal-testing-requirement-monoclonal-antibodies-and-other-drugs

Ban K, Bae S, Yoon YS. 2017. Current strategies and challenges for purification of cardiomyocytes derived from human pluripotent stem cells. Theranostics. 7(7):2067–2077. https://doi.org/10.7150/thno.19427

Boheler KR, Poon EN. 2021. Cell surface markers for immunophenotyping human pluripotent stem cell-derived cardiomyocytes. Pflügers Archiv - Euro J Physiol. 473(7):1023–1039. https://doi.org/10.1007/s00424-021-02549-8

Cai W et al. 2019. An unbiased proteomics method to assess the maturation of human pluripotent stem cell-derived cardiomyocytes. Circ Res. 125(11):936–953. https://doi.org/10.1161/CIRCRESAHA.119.315305

Deuse T et al. 2021. The SIRPα–CD47 immune checkpoint in NK cells. J Exp Med. 218(3):936–953. https://doi.org/10.1084/jem.20200839
Dubois NC et al. 2011. SIRPA is a specific cell-surface marker for isolating cardiomyocytes derived from human pluripotent stem cells. Nat Biotechnol. 29(11):1011–1018. https://doi.org/10.1038/nbt.2005
Funakoshi S et al. 2021. Generation of mature compact ventricular cardiomyocytes from human pluripotent stem cells. Nat Commun. 12(1):3155. https://doi.org/10.1038/s41467-021-23329-z
Gao Y et al. 2023. Ascorbic acid induces MLC2v protein expression and promotes ventricular-like cardiomyocyte subtype in human induced pluripotent stem cells derived cardiomyocytes. Theranostics. 13(11):3872–3896. https://doi.org/10.7150/thno.80801
Giacomelli E et al. 2020. Human-iPSC-derived cardiac stromal cells enhance maturation in 3D cardiac microtissues and reveal non-cardiomyocyte contributions to heart disease. Cell Stem Cell. 26(6):862–879.e11. https://doi.org/10.1016/j.stem.2020.05.004
Guo Y, Pu WT. 2020. Cardiomyocyte maturation. Circ Res. 126(8):1086–1106. https://doi.org/10.1161/CIRCRESAHA.119.315862
Kadari A et al. 2015. Robust generation of cardiomyocytes from human iPS cells requires precise modulation of BMP and WNT Signaling. Stem Cell Reviews and Reports. 11(4):560–569. https://doi.org/10.1007/s12015-014-9564-6
Karbassi E et al. 2020. Cardiomyocyte maturation: advances in knowledge and implications for regenerative medicine. Nat Rev Cardiol. 17(6):341–359. https://doi.org/10.1038/s41569-019-0331-x
Laco F et al. 2020. Selection of human induced pluripotent stem cells lines optimization of cardiomyocytes differentiation in an integrated suspension microcarrier bioreactor. Stem Cell Res Ther. 11(1):118. https://doi.org/10.1186/s13287-020-01618-6
Paakkari I. 2002. Cardiotoxicity of new antihistamines and cisapride. Toxicol Lett. 127(1-3):279–284. https://doi.org/10.1016/s0378-4274(01)00510-0
Park SJ et al. 2025. Stage-specific cardiotoxicity induced by bisphenol A using human pluripotent stem cell-derived 2D- and 3D-cardiomyocyte models. J Tissue Eng. 16:20417314251383006. https://doi.org/10.1177/20417314251383006
Ronaldson-Bouchard K et al. 2018. Advanced maturation of human cardiac tissue grown from pluripotent stem cells. Nature. 556(7700):239–243. https://doi.org/10.1038/s41586-018-0016-3
Rupert CE, Irofuala C, Coulombe KLK. 2020. Practical adoption of state-of-the-art hiPSC-cardiomyocyte differentiation techniques. PLoS One. 15(3):e0230001. https://doi.org/10.1371/journal.pone.0230001
Selvakumar D et al. 2024. Cellular heterogeneity of pluripotent stem cell-derived cardiomyocyte grafts is mechanistically linked to treatable arrhythmias. Nat Cardiovasc Res. 3(2):145–165. https://doi.org/10.1038/s44161-023-00419-3
Sharifi-Sanjani M et al. 2014. Cardiac CD47 drives left ventricular heart failure through Ca^{2+}-CaMKII-regulated induction of HDAC3. J Am Heart Assoc. 3(3):e000670. https://doi.org/10.1161/JAHA.113.000670
Skelton RJ et al. 2014. SIRPA, VCAM1 and CD34 identify discrete lineages during early human cardiovascular development. Stem Cell Res. 13(1):172–179. https://doi.org/10.1016/j.scr.2014.04.016
Tohyama S et al. 2013. Distinct metabolic flow enables large-scale purification of mouse and human pluripotent stem cell-derived cardiomyocytes. Cell Stem Cell. 12(1):127–137. https://doi.org/10.1016/j.stem.2012.09.013
Uosaki H et al. 2011. Efficient and scalable purification of cardiomyocytes from human embryonic and induced pluripotent stem cells by VCAM1 surface expression. PLoS One. 6(8):e23657. https://doi.org/10.1371/journal.pone.0023657
Veevers J et al. 2018. Cell-surface marker signature for enrichment of ventricular cardiomyocytes derived from human embryonic stem cells. Stem Cell Rep. 11(3):828–841. https://doi.org/10.1016/j.stemcr.2018.07.007
Waring MJ et al. 2015. An analysis of the attrition of drug candidates from four major pharmaceutical companies. Nat Rev Drug Discovery. 14(7):475–486. https://doi.org/10.1038/nrd4609